Received: 27 April 2021 | Revised: 17 May 2021 | Accepted: 18 May 2021

DOI: 10.1002/jgm.3365

RESEARCH ARTICLE

WILEY

Hsa_circRNA_102229 facilitates the progression of triple-negative breast cancer via regulating the miR-152-3p/PFTK1 pathway

Chuang Du | Jianhua Zhang | Linfeng Zhang | Yingying Zhang | Yan Wang | Jingruo Li

Department of Breast Surgery, The First Affiliated Hospital of Zhengzhou University, Zhengzhou City, Henan Province, China

Correspondence
Jingruo Li, Department of Breast Surgery, The First Affiliated Hospital of Zhengzhou University, No. 1, Jianshe East Road. Zhengzhou City, Henan Province, China.
Email: jrli999@163.com

Funding information
Joint Project of Henan Province and Ministry, Grant/Award Number: 2018010002; Guidance Plan of Key Scientific Research Projects in Henan Province, Grant/Award Number: 20B320026; Joint Construction Project of Henan Medical Science and Technology Research Plan, Grant/Award Number: LHGJ20190146

Abstract

Background: Increasing evidence has suggested that circular RNAs (circRNAs) may act as an important regulatory factor in tumor progression. However, how circRNAs exert their functions in triple-negative breast cancer (TNBC) remains not clearly understood.

Methods: First, circRNA microarrays were conducted to identify aberrantly expressed circRNAs in TNBC tissues. Kaplan–Meier survival analysis was conducted to calculate the correlation between the level of hsa_circRNA_102229 and outcomes of patients with TNBC. The effect of hsa_circRNA_102229 and serine/threonine-protein kinase PFTAIRE 1 (PFTK1) on TNBC cells was clarified by cell counting kit-8, transwell and wound healing assays, as well as by a flow cytometry. The molecular mechanism of hsa_circRNA_102229 was clarified through bioinformatics, a dual-luciferase reporter assay, western blotting, fluorescence *in situ* hybridization and real-time polymerase chain reaction. Tumor xenograft experiments were performed to analyze growth and metastasis of TNBC *in vivo*.

Results: In TNBC tissues and cells, hsa_circ_102229 was remarkably up-regulated. Patients with TNBC presenting high hsa_circ_102229 exhibited poor prognosis. Moreover, hsa_circ_102229 could promote the migration, proliferation and invasion, whereas it inhibited the apoptosis of TNBC cells. Furthermore, hsa_circ_102229 directly targeted miR-152-3p and could regulate the expression of PFTK1 by targeting miR-152-3p. Rescue assays suggested that hsa_circ_102229 may exert its function in TNBC cells by regulating PFTK1. Additionally, knockdown of hsa_circ_102229 slowed down TNBC tumorigenesis and lung metastasis in a tumor xenograft animal model.

Conclusions: Hsa_circ_102229 might serve as a competing endogenous RNA (ceRNA) to modulate PFTK1 expression via regulating miR-152-3p to affect the functions of TNBC cells. Hsa_circ_102229 acts as a newly discovered biomarker for TNBC treatment.

KEYWORDS
hsa_circRNA_102229, miR-152-3p, PFTK1, prognosis, triple-negative breast cancer

1 | INTRODUCTION

In recent years, breast cancer has increasingly become the most prevalent cancer affecting females worldwide and has caused great morbidity and mortality.[1,2] Among total cancer cases, breast cancer accounts for 23%, and the predicted incidence will reach to round 3.2 million cases per year by 2050.[3] Although great achievements have been made in terms of technological advances on early diagnosis and treatment, the aggressiveness of this disease is still difficult to prevent.[4] Thus, the molecular mechanisms underlying the progress of breast cancer are worthy of exploration.

As a molecularly heterogeneous disease, breast cancer can be categorized into five different subtypes according to the level of progesterone receptors (PR), estrogen receptors (ER) and the epidermal growth factor receptor 2 (HER2) oncogene.[5,6] One type that does not express either PR, ER or HRE2 are the triple-negative breast cancers (TNBC),[6,7] which are considered to be most aggressive, accounting for approximately 15% of breast cancers.[8] At present, the treatment response and outcomes of patients with TNBA have been confirmed to be worse than for patients with other subtypes.[9–11] Until now, there are no advanced treatment options available for TNBC.[12]

As a newly discovered endogenous non-coding RNA, circular RNA (circRNA) usually consists of more than one hundred nucleotides.[13,14] Previously, circRNAs were identified and considered to have a lack of biological functions in many types of species.[15] In recent years, with the development of deep sequencing technology, numerous of circRNAs have been found play essential roles in the physiological processes of mammalian cells.[16–18] It is reported that circRNAs were greatly involved in progression of different tumors and, in some cases, might play opposite roles.[19] For example, circRNA_102171 was confirmed to enhance the progression of papillary thyroid cancer[20]; however, the progression of lung cancer can be largely inhibited by hsa_circ_100395.[21] In TNBC, there were already many circRNAs that were confirmed to play critical roles in pathophysiological process in different stages.[22] For example, circEPSTI1 affected the proliferation and apoptosis of TNBC cells, thus serving as a mediator of TNBC progression.[23] The levek of another circRNA, named circAGFG1, was correlated with poor outcomes in patients with TNBC, and circAGFG1 could promote tumorigenesis and metastasis of TNBC.[24] However, for most newly discovered circRNAs, the underlying molecular mechanisms with respect to TNBC progression remain not clearly understood.

In the present study, using microarray analysis, we discovered that hsa_circRNA_102229 was highly expressed in TNBC tissues. Furthermore, Kaplan–Meier analysis clarified that the expression of hsa_circRNA_102229 was correlated with clinical outcome of patients with TNBC. Thus, the present study aimed to identify the role of hsa_circRNA_102229 in TNBC and then investigate its down-stream factors and mechanisms with respect to TNBC progression. The results might provide a novel sight into the pathophysiologic mechanisms of TNBC progression and, more importantly, might also provide a new theoretical basis for the therapeutic targeting of TNBC treatment.

2 | MATERIALS AND METHODS

2.1 | Microarray analysis and bioinformatic analysis

Datasets of microarray analysis were obtained from the GEO database (http://www-ncbi-nlm-nih-gov.ezproxy.lb.polyu.edu.hk/geo) with accession number GSE101123. Differently expressed circRNAs were defined with $p < 0.05$. Starbase (http://starbase.sysu.edu.cn) was used for detecting the potential binding sites between miR-152-3p and hsa_circRNA_102229 or serine/threonine-protein kinase PFTAIRE 1 (PFTK1).

2.2 | TNBC samples and cells

Human related experiments were approved by the Ethical Committee of The First Affiliated Hospital of Zhengzhou University (approval no. 2019-KY-291). TNBC patient samples and corresponding adjacent breast tissues were obtained from patients with breast resection at The First Affiliated Hospital of Zhengzhou University. Written consent of all TNBC patients was obtained prior to conducting research related procedures. No TNBC patients had received any special treatment before the breast resection. Obtained tissues were maintained at −80°C followed by snap-freezing in liquid nitrogen.

Human TNBC cell lines (SUM149PT, SUM159PT, MDA-MB-231, MDA-MB-468) and parallel cell line (MCF10A) were obtained from American Type Culture Collection (Manassas, VA, USA). All types of cells were cultured with Dulbecco's modified Eagle's medium (Invitrogen, Carlsbad, CA, USA) with a combination of penicillin/streptomycin (1%) (Invitrogen) and 10% fetal bovine serum (FBS) (Carlsbad, CA, USA).

2.3 | RNase R treatment

For the RNase R related procedure, RNAs extracted from TNBC cells were treated with 3 U μg^{-1} RNase R for 15 min at 37°C. Then, a quantitative real-time polymerase chain reaction (qRT-PCR) was performed. The level of circRNA and liner mRNA were determined.

2.4 | qRT-PCR

We isolated total RNA from TNBC tissues and TNBC cultured cells using Trizol reagent (Life Technologies, Carlsbad, CA, USA). Then, PrimeScript RT reagent kit (Takara Biotechnology, Shiga, Japan) was used for synthesizing first-strand cDNAs. The reverse process of miRNA was performed using a MicroRNA Reverse Kit (Takara Biotechnology). After completing the reverse transcription of total RNA and miRNA, qPCR was conducted on an ABI 7500 Fast system (Thermo Fisher Scientific, Walthem, MA, USA) using a SYBR Green PCR Master Mix (Applied Biosystems). Detailed information on the primers used in the current experiments is provided in Table 1.

2.5 | *In situ* hybridization (ISH)

Manual tissue microarrayer (Beecher Instruments, Sun Prarie, WI, USA) was used for TMA (triplicate 0.6-mm cores). Then, hsa_circRNA_102229 was labeled with digoxin-labeled RNA probe (BOSTER, Wuhan, China). Positive control and negative control probe were run on each tissue prior to testing with the hsa_circRNA_102229 probe. After incubating with antibody against digoxigenin, TMA was hybridized with the hsa_circRNA_102229 probe, as well as its positive control and negative control. Subsequently, the results were measured using diaminobenzidine (DAB) solution. The sequences of the probes were: hsa_circRNA_102229 probe: 5′-AGCAGAACAGGATCTATGCCAT-3′ and scramble probe: 5′-GTGTAACACGTCTATACGCTCA-3′.

2.6 | TNBC cell transfection

miR-152-3p mimic, inhibitor and their control plasmids (NC mimic, NC inhibitor), short hairpin RNA (shRNA) targeting hsa_circRNA_102229 (sh-NC as its negative control), and pcDNA3.1(+) vectors for overexpressing hsa_circRNA_102229 and PFTK1 or their negative controls (vector, vehicle) were purchased from Sigma-Aldrich (St Louis, MO, USA). The transfection process was performed using Lipofectamine 3000 (Invitrogen). The circRNAsh sequences were: circRNAsh1#: CCGGCGTCCGCTACAGTCGAAATAACTCG; circRNAsh2#: CCGGCGGAAGG-. TTGGCTGGATATTTCTCGA GAAATATC.

TABLE 1 Primers used in the present study

Gene	Primer sequence
hsa_circ_102229	Forward: 5′-ATAAAGRGCRGACAGTGCAGATAGTG-3′
	Reverse: 5′-TCAAGTACCCACAGTGCGGT-3′
miR-152-3p	Forward: 5′-CTAGTCCAGTTTTCCCAGGA-3′
	Reverse: 5′-CAGTGCGTGTCGTGGAGT-3′
U6	Forward: 5′-CTCGCTTCGGCAGCACA-3′
	Reverse: 5′-AACGCTTCACGAATTTGCGT-3′
PFTK1	Forward: 5′-TGAAGCTGGCAGATTTCGGT-3′
	Reverse: 5′-GTGGAGGCAGATCGCTGAAA-3′
GAPDH	Forward: 5′-CCGGGAAACTGTGGCGTGATGG-3′
	Reverse: 5′-AGGTGGAGGAGTGGGTGTCGCTGTT-3′

2.7 | Cell counting kit (CCK)-8 assay

For the CCK-8 assay, briefly, after seeding the TNBC cells in a 96-well plate, 10 μl of CCK-8 reagent was added and co-incubated with transfected TNBC cells. The optical density (OD) was determined at 450 nm using a microplate reader (Männedorf, Zurich, Switzerland).

2.8 | 5-Ethynyl-2′-deoxyuridine (EdU) staining

Different group of TNBC cells, at a density of 1×10^5 cells/well, were washed and then fixed with 4% paraformaldehyde for 10 min. Afterwards, 20 μM EdU reagent was added to the culture medium for treating TNBC cells. Then, cells were kept from lights at room temperature. Finally, 4′,6-diamidino-2-phenylindole (DAPI) was used for nuclei staining.

2.9 | Flow cytometry

The apoptosis of different groups of TNBC cells was detected by flow cytometry analysis. Briefly, at room temperature, after suspension in 500 μl of flow cytometry binding buffer, transfected TNBC cells were labeled with the same volume of annexin V/fluorescein isothiocyanate (FITC) or propidium iodide (PI) in the dark for 20 min. Signals were detected and then analyzed.

2.10 | Cell migration measurement

The migration ability of different group of TNBC cells was examined using a wound-healing assay. Briefly, TNBC cells were cultured on a six-well plate. After growing to approximately 80% confluence, a monolayer of cells was wounded by a pipette tip (200 μl). At 0 and 24 hours, the movement of differents group of TNBC cells was recorded under an microscope (Olympus, Tokyo, Japan).

2.11 | Transwell assay

Briefly, 100 μl cell suspension was seeded into upper chamber coated with 30 μ; of matrigel and 800 μl of medium supplemented with 1%

FBS was added into the lower chamber. After 24 hours, Giemsa (#10092-013; Gibco, Gaithersburg, MD, USA) was used for staining the invaded cells.

2.12 | Immunofluorescence

N-cadherin and E-cadherin was detected in different groups of transfected TNBC cells. Transfected TNBC cells were fixed with 4% paraformaldehyde solution. After blocking, sections were incubated overnight with primary antibodies, including N-cadherin (#ab76057; dilution 1:1000; Abcam, Cambridge, MA USA) antibodies and E-cadherin (#ab194982; dilution 1:1000; Abcam) at 4°C. Next, sections were incubated with Alexa-conjugated anti-goat (Alexa647; Invitrogen) or FITC-conjugated anti-rabbit secondary antibody (FITC; Invitrogen), for 1 hour. In the end, transfected TNBC cells were stained with DAPI (dilution 1:1000; Beyotime, Nanjing, China).

2.13 | Dual-luciferase reporter assay

Putative wild-type (wt) and mutant (mut) miR-152-3p binding sites of hsa_circRNA_102229 (circRNA-wt, circRNA-mut) and PFTK1 (PFTK1-wt, PFTK1-mut) were cloned into a pmirGLO-Report luciferase vector (Promega, Madison, WI, USA) and co-transfected with NC mimics or miR-152-3p mimics via Lipofectamine 3000 (Invitrogen).

2.14 | Fluorescence *in situ* hybridization (FISH)

Cy3-labeled probes for detecting miR-152-3p and Fluor 633-labeled probe for observing hsa_circRNA_102229 were synthesized by GenePharma (Shanghai, China). Pre-hybridization buffer was added into different groups of cells. Afterwards, hybridization was performed at 55°C for 2 hours. DAPI was used to label nuclei. The probe signals were investigated using a FISH Kit (RiboBio, Guangzhou, China) in accordance with the manufacturer's instructions.

2.15 | Western blotting

Transfected TNBC cells were lysed in 100 μl of lysis buffer for 20 min on ice. After concentration detection, protein was loaded onto 10–15% sodium dodecyl sulfate gel and fractionated onto polyvinylidene difluoride membranes (Burlington, MA, USA). The membranes were then washed with Tris-buffered saline-Tween 20 and, after blocking with skim milk, the membranes were incubated with primary antibodies: anti-PFTK1 (#ab224098; dilution 1:1000; Abcam), GADPH (#ab8245; dilution 1:1000; Abcam). Then, at room temperature, the secondary antibodies (dilution 1:2000) were added onto the membranes for 60 min. Images were recorded and the data were analyzed using ImageJ (NIH, Bethesda, MD, USA).

2.16 | *In vivo* animal model

MDA-MB-468 cells transfected with sh-hsa_circRNA_102229 or sh-NC were re-suspended and subcutaneously injected into the right flank of the nude mice (male BALB/c nude mice, 4–5 weeks old, $n = 6$ each group). The volume of the tumors was recorded every 2 days, 1 week after the first injection. After mice were sacrificed, tumors were collected and weighed. MDA-MB-468 cells transfected with sh-hsa_circRNA_102229 or sh-NC were labelled with luciferase labelled for metastasis detection. Next, these cells were tail-vein injected into the nude mice ($n = 6$ each group). Progression of tumors and lung metastases was determined using the IVIS 100 Imaging System (Xenogen, Princeton, NJ, USA). Monological experiments were performed using hemotoxylin and eosin staining. Animal-related experiments were approved by the Ethical Committee of The First Affiliated Hospital of Zhengzhou University (approval no. 2019-KY-291).

2.17 | Terminal deoxynucleotidyl transferase (TdT) dUTP nick-end labeling (TUNEL) assay

Briefly, the paraffin sections from different groups of mice were digested with proteinase K in Tris/HCl buffer containing ethylenediaminetetraacetic acid. Afterwards, terminal deoxyribonucleotidyl transferase (75 U/ml) and digoxigenin11-dUTP were added. After the alkaline phosphatase reaction, sections were counterstained with hematoxylin.

2.18 | Immunohistochemistry assay (IHC)

Before IHC, tissue sections originally from xenograft tumor were fixed by formalin and embedded into paraffin. Subsequently, primary antibodies were added and co-incubated with tissue sections, including anti-E-cadherin (#ab1416; dilution 1:500; Abcam), anti-PFTK1 (#ab224098; dilution 1:1000; Abcam) anti-Ki67 (#ab245113; dilution 1:1000; Abcam), antibodies. Sections were then incubated with horseradish peroxidase-polymer-conjugated secondary antibody at 37°C for 1 hour after washing with phosphate-buffered saline. Finally, sections were immunostained with a DAB plus kit (BioDee, Beijing, China).

2.19 | Statistical analysis

All error bars indicate the SD. A Student's *t* test and one-way analysis of variance were used for two-sample comparisons and multiple-sample

comparisons, respectively, followed by Bonferroni's multiple comparison test. SPSS, version 21.0 (IBM Corp., Armonk, NY, USA) was used to conduct the statistical analysis. Survival curves were evaluated by Kaplane–Meier analysis. The Pearson correlation coefficient was used for correlation analysis. $p < 0.05$ was considered statistically significant. Cell experiments were performed in triplicate.

3 | RESULTS

3.1 | Hsa_circ_102229 was increasingly expressed in TNBC tissues and breast cancer cells

First, datasets of microarray analysis of GSE101123 were collected and analyzed. The volcano plot is shown in Figure 1A. Down-regulated or up-regulated genes were labeled blue or red, respectively. We selected 10 differently expressed circRNAs from Figure 1A. The heatmap of these circRNAs in eight tumor samples and three normal samples is shown in Figure 1B. Among all of the differently expressed circRNAs, hsa_circ_102229 had the highest expression. Therefore, we selected hsa_circ_102229 as a candidate for further experiments. Then, the level of hsa_circ_102229 was measured in 72 pairs of TNBC and corresponding normal samples. In Figure 1C, the level of hsa_circ_102229 was remarkably elevated in TNBC samples compared to control samples ($p < 0.001$). Additionally, a high level of hsa_circ_102229 was correlated with a lower survival rate of patients with TNBC ($p = 0.0144$) (Figure 1D). Furthermore, the level of hsa_circ_102229 was associated with several clinical features (e.g. lymph node metastasis, tumor size and TNM stage), suggesting that high expression of hsa_circ_102229 was associated

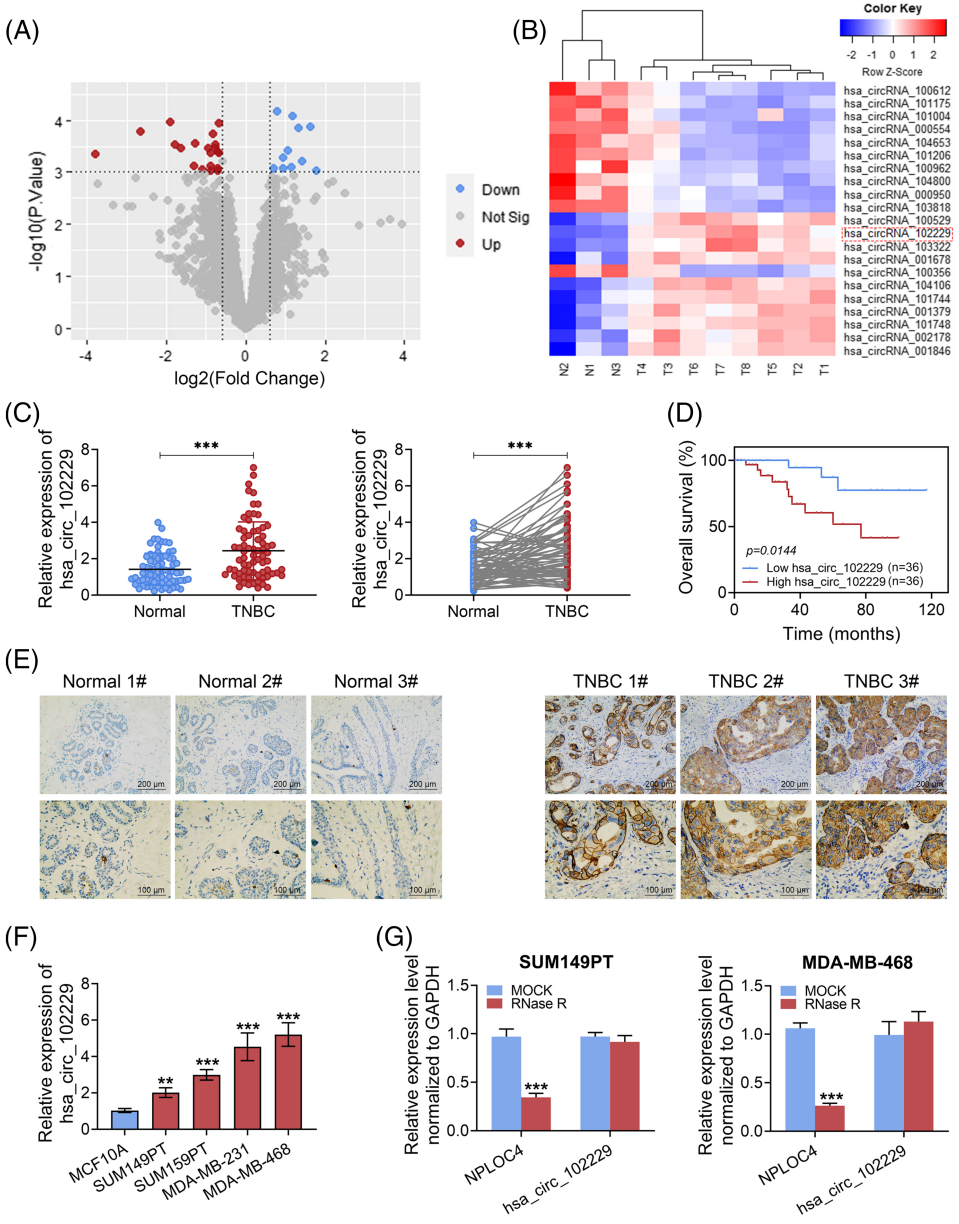

FIGURE 1 Hsa_circ_102229 was highly expressed in TNBC tissues and cells. (A) A volcano plot revealed the up-regulated (red) and down-regulated (blue) genes in TNBC patients. The data sets were obtained from GEO (GSE101123). (B) Heatmap of differently expressed circRNAs from eight TNBC tumor samples and three normal samples. (C) The expression of hsa_circ_102229 in TNBC samples ($n = 72$) and corresponding normal controls ($n = 72$) was determined by qRT-PCR. (D) Kaplan–Meier analysis exhibited the survival rate (up to 120 months) of TNBC patients with high or low expression levels of hsa_circ_102229. The high or low expression of hsa_circ_102229 was defined by the median. (E) The expression of hsa_circ_102229 in different stages (stages I–III) of TNBC in human tissue is shown using ISH. Scale bar = 200 μm (F) The hsa_circ_102229 expression levels in TNBC cell lines (SUM149PT, SUM159PT, HCC1806, MDA-MB-231, MDA-MB-468) and parallel cell line (MCF10A) were analyzed by qRT-PCR. (G) NPLOC4 mRNA and circular has_ circ_102229 were detected, and RNA samples were treated with RNase R or mock treated without the enzyme. The experiments were performed using qRT-PCR. Data are expressed as the mean ± SD. $^{**}p < 0.01$ and $^{***}p < 0.001$ represent a statistically significant difference

TABLE 2 Relationship between hsa_circ_102229 and clinic-pathological parameters

Parameters	Number of patients	Has_circ_102229 expression		*p* value
		Low (< median)	High (> median)	
Number	72	36	36	
Age (years)				
< Mean (40)	25	13	12	0.804
> Mean (40)	47	23	24	
Menopause				
Yes	31	17	14	0.475
No	41	19	22	
Tumor size				
< 2 (cm)	30	20	10	0.017*
> 2 (cm)	42	16	26	
Lymph node metastasis				
Negative	27	18	9	0.028*
Positive	45	18	27	
TNM stage				
I	20	14	6	0.029*
II	31	16	15	
III	21	6	15	
Histological grade				
I	15	10	5	0.067
II	32	18	14	
III	25	8	17	

with the poor prognosis of patients with TNBC ($p < 0.05$) (Table 2). ISH experiments demonstrated that hsa_circ_102229 was up-regulated in different stages of TNBC (Figure 1E). In addition, the relative expression of hsa_circ_102229 was examined in different TNBC cell lines (SUM149PT, SUM159PT, MDA-MB-231 and MDA-MB-468). Meanwhile, normal breast cell line MCF10A was also included. As shown in Figure 1F, the level of hsa_circ_102229 in breast cancer cell lines was significantly higher than that in normal breast cell lines ($p < 0.01$, $p < 0.001$), especially in MDA-MB-468 cells. We selected SUM149PT and MDA-MB-468 cells to perform further experiments. Finally, the expression of linear NPLOC4 mRNA and circular hsa_circ_102229 was clarified in SUM149PT and MDA-MB-468 cell lines, respectively. It was shown that hsa_circ_102229 was not affected by Rnase R, suggesting that hsa_circ_102229 was circRNA, and not linear RNA ($p < 0.001$) (Figure 1G). Taken together, the above results demonstrated that the level of hsa_circ_102229 was dramatically increased in TNBC; moreover, its expression was strongly associated with the negative outcomes of patients with TNBC.

3.2 | Hsa_circ_102229 enhanced the proliferation and suppressed the apoptosis of TNBC cells

Hsa_circ_102229 overexpression and a knockdown system were established via pcDNA3.1(+) hsa_circ_102229 vector and lentivirus-mediated shRNA target hsa_circ_102229 (circRNAsh1#, circRNAsh2#) in SUM149PT and MDA-MB-468 cell lines, respectively. The results showed that these systems were successfully constructed ($p < 0.01$, $p < 0.001$) (Figure 2A). Afterwards, a CCK-8 assay and EdU staining were conducted to determine the proliferation of TNBC cells. The results demonstrated that overexpression of hsa_circ_102229 elevated the proliferation of TNBC cells ($p < 0.05$, $p < 0.01$) (Figure 2B and 2C), whereas knockdown of hsa_circ_102229 inhibited cell proliferation ability ($p < 0.05$, $p < 0.01$) (Figure 2B and 2C). In addition, the effect of hsa_circ_102229 on TNBC cells apoptosis was detected by flow cytometry assay. The percentage of apoptosis was decreased upon overexpression of hsa_circ_102229 in SUM149PT cells ($p < 0.05$) (Figure 2D). However, knockdown of hsa_circ_102229 significantly enhanced the apoptosis rate of MDA-MB-468 cells ($p < 0.01$) (Figure 2D).

3.3 | Hsa_circ_102229 improved the migration and invasion abilities of TNBC cells

Furthermore, the effect of overexpression or knockdown of hsa_circ_102229 on cell migration and invasion was analyzed. The results showed that overexpressed hsa_circ_102229 dramatically promoted the migration and invasion of SUM149PT cells ($p < 0.01$) (Figure 3A and 3B). Correspondingly, knockdown of hsa_circ_102229

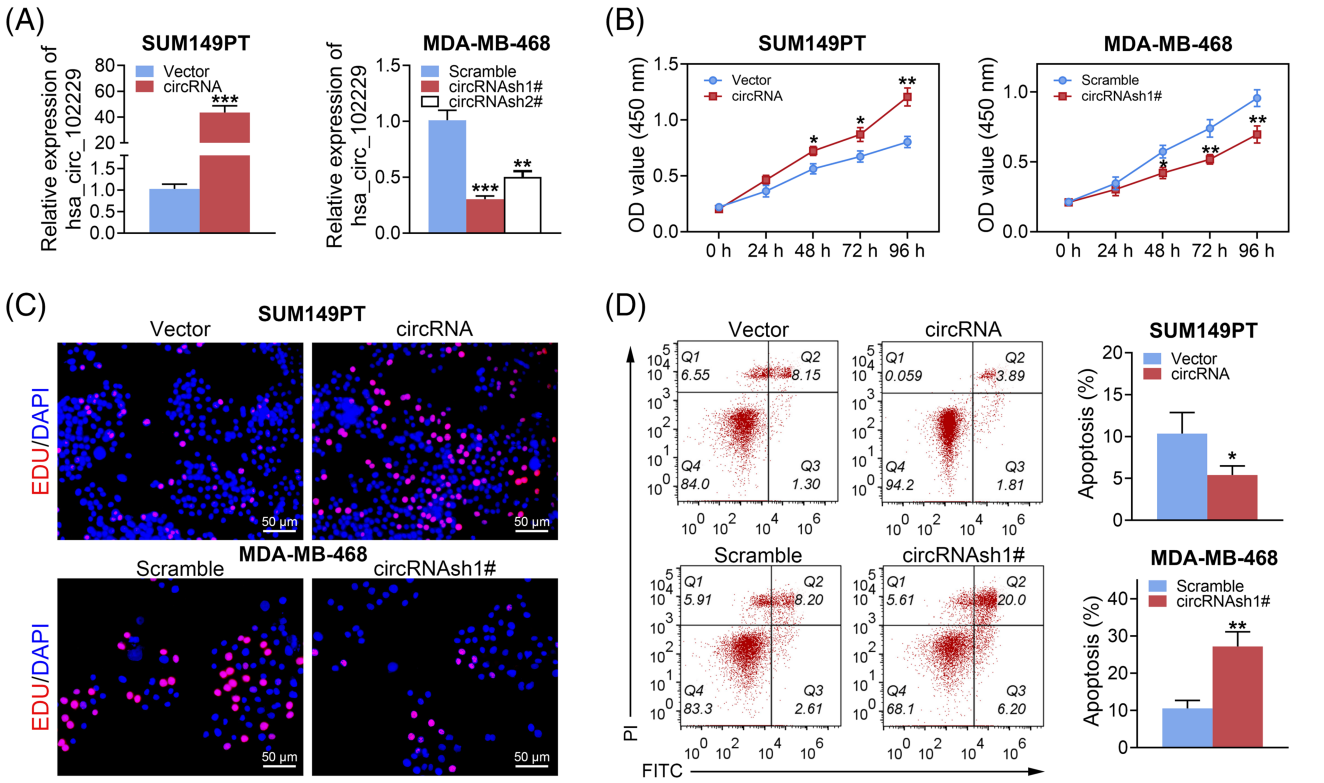

FIGURE 2 Hsa_circ_102229 promoted the proliferation and inhibited the apoptosis of TNBC cells. (A) The expression level of hsa_circ_102229 were determined by qRT-PCR in SUM149PT and MDA-MB-468 cells transfected with pcDNA3.1(+) hsa_circ_102229 vector (circRNA) or lentivirus-mediated short hairpin RNA (shRNA) target hsa_circ_102229 (circRNAsh1#, circRNAsh2#), respectively. (B) Growth curves were analyzed by the CCK-8 assay in SUM149PT or MDA-MB-468 cell transfection with circRNA (control: Vector) or circRNAsh1# (control: Scramble) for 0, 24, 48, 72 and 96 hours. (C) The effect of overexpressed hsa_circ_102229 or hsa_circ_102229 knockdown on cells proliferation was determined by EdU staining using SUM149PT or MDA-MB-468 cell lines, respectively. (D) The effects of overexpressed hsa_circ_102229 or knockdown hsa_circ_102229 on cell apoptosis were determined by flow cytometry on SUM149PT or MDA-MB-468 cell lines, respectively. Data are expressed as the mean ± SD. $^{*}p < 0.05$, $^{**}p < 0.01$ and $^{**}p < 0.001$ represent a statistically significant difference

significantly inhibited the migration and invasion of MDA-MB-468 cells ($p < 0.05$, $p < 0.01$) (Figure 3A and 3B). Additionally, the level of N-cadherin and E- cadherin was clarified using immunofluorescence. In Figure 3C, overexpression of hsa_circ_10222 is seen to enhance the expression of N-cadherin, but suppress the expression of E-cadherin, whereas knockdown of hsa_circ_10222 has the opposite effect. Quantitative data are shown in the Supporting information (Figure S1). Moreover, a series of experiments were conducted to confirm that there were no off-target effects (see Supporting information, Figure S2). In sum, these findings revealed that hsa_circ_102229 promoted the migration and invasion of TNBC cells.

3.4 | Hsa_circ_102229 bound and negatively regulated the level of miR-152-3p

To further investigate the underlying mechanism of hsa_circ_102229 on TNBC, bioinformatic analysis was introduced. Using Starbase (http://starbase.sysu.edu.cn), we found that miR-152-3p contains the potential binding sites for hsa_circ_102229 (Figure 4A). Hsa_circ_102229 wild-type (wt) or mutated (mut), containing the potential miR-152-3p binding sites, was co-transfected with miR-152-3p mimic or miR-NC. As shown in Figure 4B, hsa_circ_102229 wt with miR-152-3p mimic group showed lower luciferase activity compared to the control ($p < 0.001$). The results of the FISH assay demonstrated that both hsa_circ_102229 and miR-152-3p were localized in the cytoplasm of TNBC cells (Figure 4C). Moreover, the relative level of miR-152-3p was detected with respect to hsa_circ_102229 overexpression or the knockdown group (Figure 4D). The results demonstrated that the expression of miR-152-3p can be inhibited by overexpressed hsa_circ_102229 ($p < 0.001$) and promoted by down-regulation of hsa_circ_10222 ($p < 0.001$). The expression of miR-152-3p was remarkably inhibited in TNBC tissue compared to that in the normal group ($p < 0.001$) (Figure 4E). In addition, correlation analysis demonstrated that the expression of hsa_circ_102229 was negatively correlated with the expression of miR-152-3p ($p < 0.001$, $r = -0.5589$). In sum, all of the results indicated that hsa_circ_102229 bound and attenuated the expression of miR-152-3p.

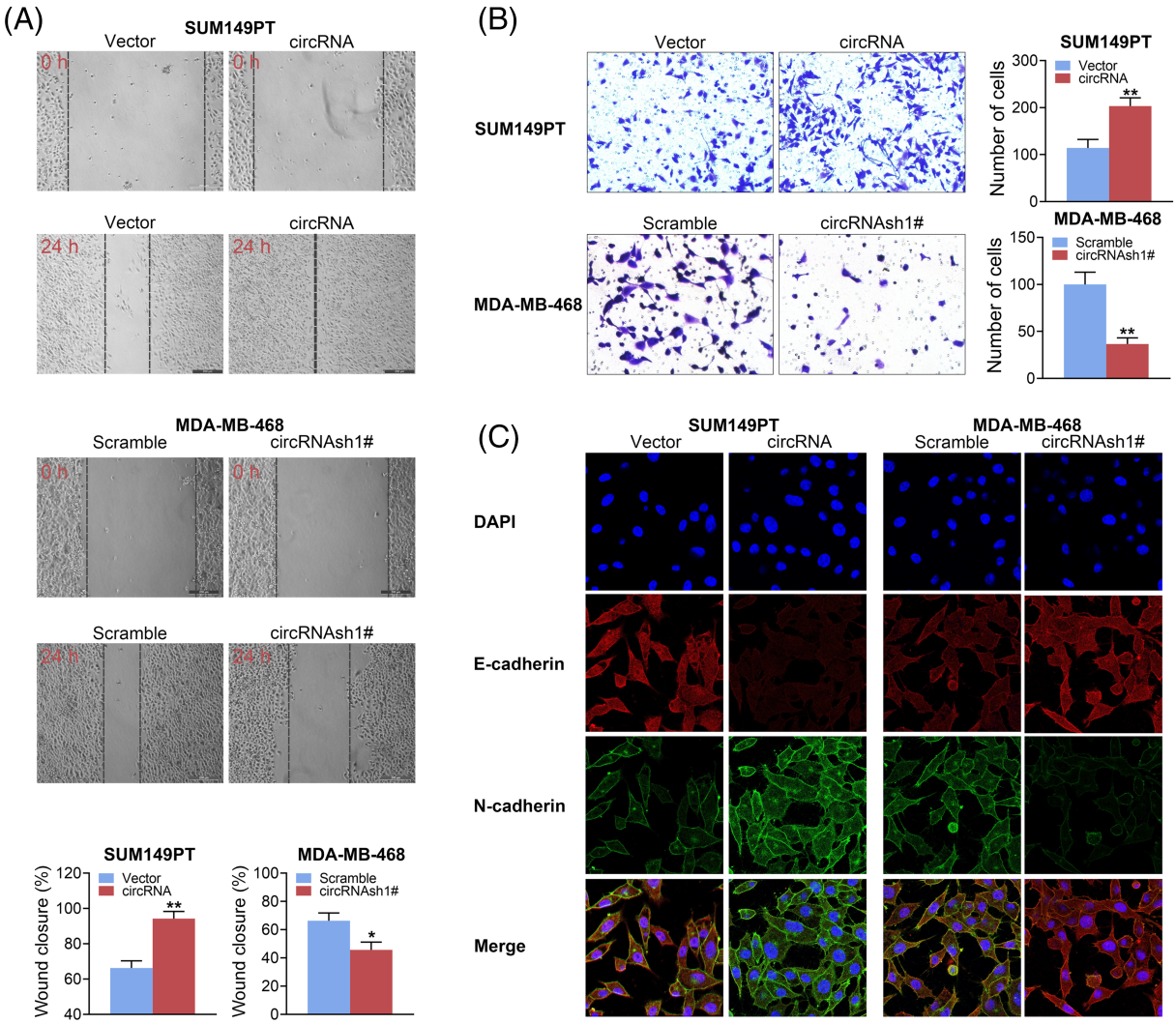

FIGURE 3 Hsa_circ_102229 promoted the migration and invasion of TNBC cells. SUM149PT and MDA-MB-468 cells were transfected with pcDNA3.1(+) hsa_circ_102229 vector (circRNA) or lentivirus-mediated short hairpin RNA (shRNA) target hsa_circ_102229 (circRNAsh1#, circRNAsh2#), respectively: (A) The effects of overexpressed hsa_circ_102229 or knockdown hsa_circ_102229 on TNBC cells migration were determined by a wound healing assay. (B) The effects of overexpressed hsa_circ_102229 or knockdown hsa_circ_102229 on TNBC cells invasion were determined by a transwell assay. (C) The expression of E-cadherin and N-cadherin in overexpressed hsa_circ_102229 or knockdown hsa_circ_102229 groups was detected by immunofluorescence. Data are expressed as the mean ± SD. $^{*}p < 0.05$ and $^{**}p < 0.01$ represent a statistically significant difference

3.5 | Hsa_circ_102229 modulated the expression of PFTK1 by targeting miR-152-3p

Furthermore, the exploration using Starbase (http://starbase.sysu.edu.cn) also suggested that PFTK1 could bind to miR-152-3p (Figure 5A). The results of the dual-luciferase reporter assay suggested that PFTK1 was a confirmed target of miR-152-3p ($p < 0.001$) (Figure 5B). Then, miR-152-3p mimic or inhibitor, as well as their corresponding controls (NC-mimic, NC-inh), were transfected into TNBC cells. The protein expression of PFTK1 was detected in each group. In Figure 5C, the expression of PFTK1 is seen to be significantly up-regulated by inhibitory of miR-152-3p ($p < 0.01$) and overexpressed miR-152-3p suppressed the expression of PFTK1 ($p < 0.001$). Moreover, the level of PFTK1 mRNA was remarkably increased in TNBC tissues compared to that in normal control ($p < 0.001$) (Figure 5D). Further results demonstrated that the expression of PFTK1 was positively correlated with the expression of hsa_circ_102229 and negatively correlated with the expression of miR-152-3p (Figure 5E). Finally, miR-152-3p mimic or its control (NC-mimic) and pcDNA3.1(+) hsa_circ_102229 or its control (vector) were co-transfected into SUM149PT cells. Meanwhile, miR-152-3p inhibitor or its control (NC-inh) and circRNAsh or its control (scramble) were co-transfected into MDA-MB-468 cells. Then, protein expression of PFTK1 was determined by western blotting. The results demonstrated that overexpression of hsa_circ_102229 elevated the expression of PFTK1, whereas this effect was reversed by overexpression of miR-152-3p ($p < 0.001$) (Figure 5F). By contrast, protein expression of PFTK1 was inhibited by knockdown of hsa_circ_102229; however, this effect

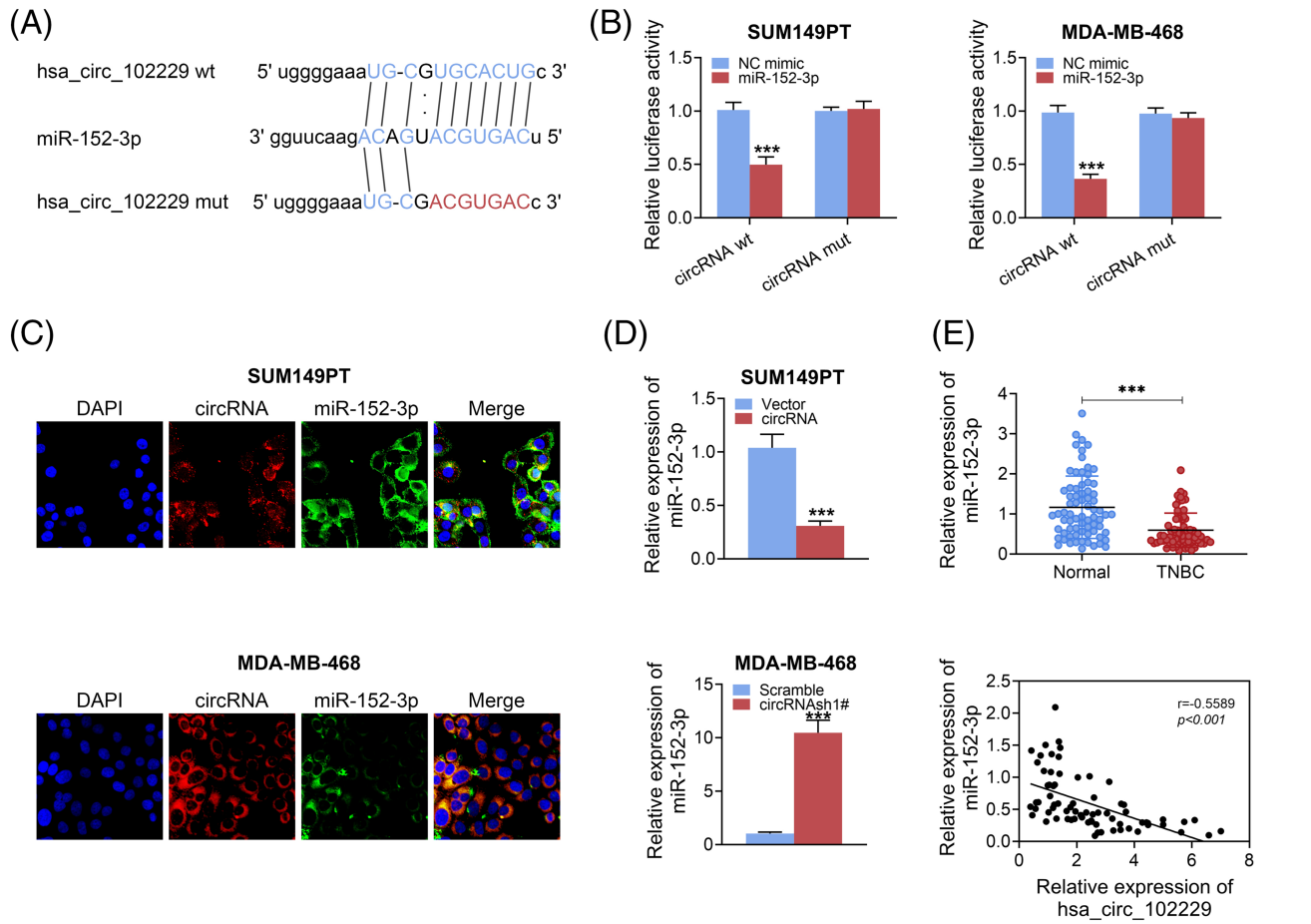

FIGURE 4 Hsa_circ_102229 bound and negatively regulated the expression of miR-152-3p. (A) Hsa_circ_102229 wide-type (wt) and mutated-type (Mut) in the miR-152-3p binding sites are shown. (B) Luciferase activity of SUM149PT and MDA-MB-468 cells co-transfected with miR-152-3p mimics or NC mimics and luciferase reporters containing hsa_circ_102229 or hsa_circ_102229 Mut transcript was tested by dual-luciferase reporter assays. (C) The localization of hsa_circ_102229 and miR-152-3p was detected by FISH in SUM149PT and MDA-MB-468 cells. (D) The effects of overexpressed hsa_circ_102229 or hsa_circ_102229 knockdown on expression of miR-152-3p were measured by qRT-PCR. (E) The expression of miR-152-3p in human TNBC samples ($n = 72$) and corresponding normal controls ($n = 72$) was determined by qRT-PCR. The correlation between expression level of hsa_circ_102229 and miR-152-3p in human TNBC tissues was analyzed. Data are expressed as the mean ± SD. $^{***}p < 0.001$ represents a statistically significant difference

could be eliminated by down-regulated miR-152-3p ($p < 0.001$) (Figure 5F). These results revealed that hsa_circ_102229 modulated the expression of PFTK1 by targeting miR-152-3p.

3.6 | Hsa_circ_102229 promoted the proliferation, migration and invasion of TNBC cells by regulating PFTK1

To better investigate the regulatory role of PFTK1 in TNBC cells, circRNAsh or its control (Scramble) and pcDNA3.1(+) PFTK1 or its control (vehicle) were co-transfected into MDA-MB-468 cells. The proliferation of MDA-MB-468 cells was investigated by the CCK-8 assay and EdU staining. It was found that knockdown of hsa_circ_102229 dramatically inhibited the cell viability and cell proliferation; however, overexpression of PFTK1 could reverse this effect ($p < 0.05$, $p < 0.01$) (Figure 6A and 6B). Moreover, apoptosis of MDA-MB-468 cells was promoted by down-regulated hsa_circ_102229 and overexpression of PFTK1 inhibited apoptosis ($p < 0.001$) (Figure 6C). In addition, different groups of MDA-MB-468 cells underwent a wound healing assay and transwell assay to measure the migration and invasion of these cells, respectively. As shown in Figure 6D,E, cell migration and invasion can be inhibited by knockdown of hsa_circ_102229 ($p < 0.01$, $p < 0.001$); however, these effects were compromised by overexpression of PFTK1. These results indicated that hsa_circ_102229 promoted the proliferation, migration and invasion of TNBC cells by regulating PFTK1.

3.7 | Knockdown of hsa_circ_102229 attenuated tumor growth and metastasis

An orthotopic xengraft mouse model was used to investigate the role of hsa_circ_102229 in tumorigenesis. Male nude mice were received

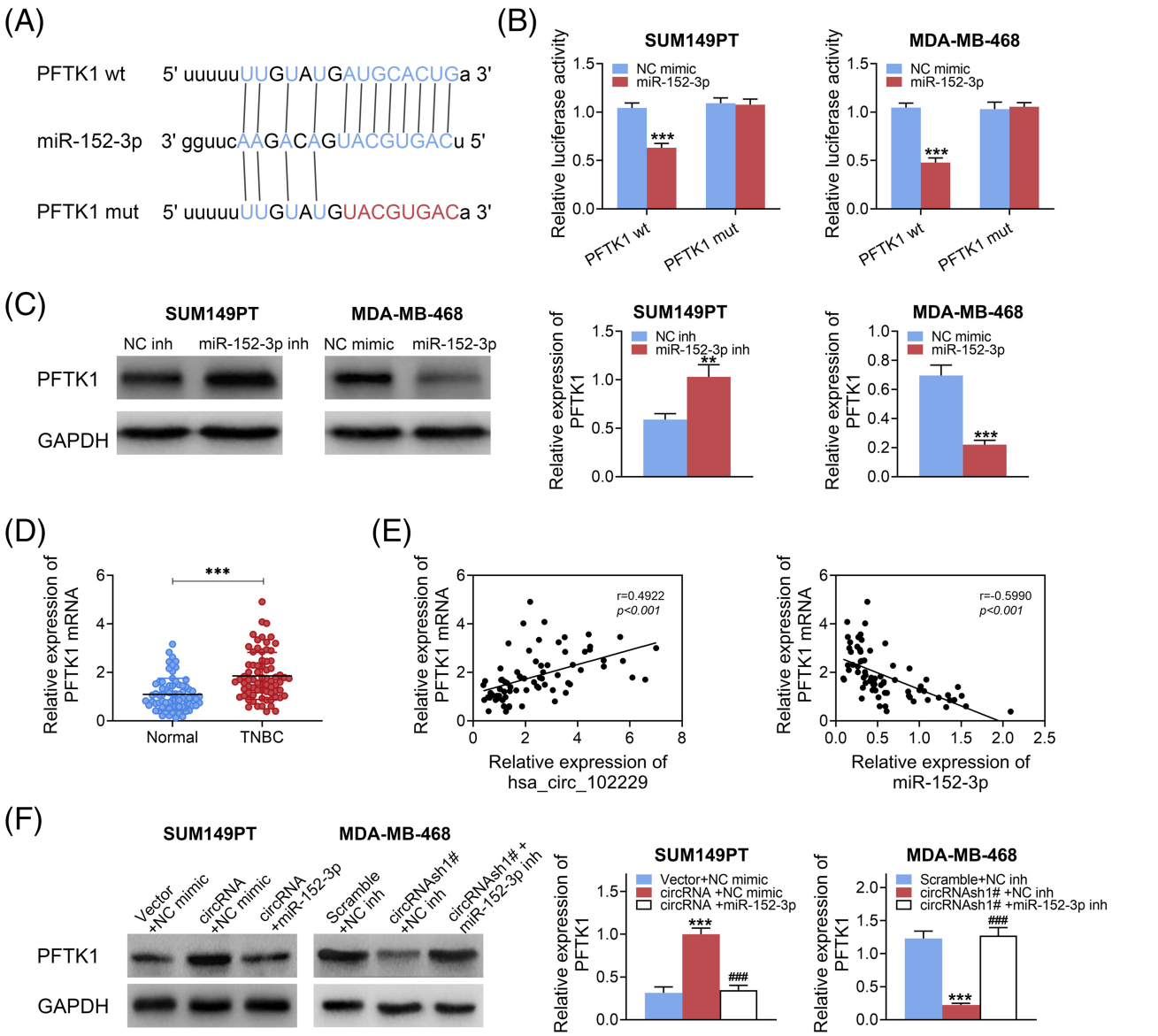

FIGURE 5 Hsa_circ_102229 regulated the expression of PFTK1 by targeting miR-152-3p. (A) PFTK1 wide-type (wt) and mutated-type (Mut) in the miR-152-3p binding sites are shown. (B) Luciferase activities of SUM149PT and MDA-MB-468 cells co-transfected with miR-152-3p mimics or NC mimics and luciferase reporters containing hsa_circ_102229 or hsa_circ_102229 Mut transcript were tested by dual-luciferase reporter assays. (C) The effect of miR-152-3p on PFTK1 expression was determined by western blotting. SUM149PT and MDA-MB-468 cells were transfected with miR-153-3p inhibitor or NC inhibitor and miR-153-3p mimic or NC mimic. (D) The expression of PFTK1 in human TNBC samples ($n = 72$) and corresponding normal controls ($n = 72$) was determined by qRT-PCR. (E) The correlation between expression level of PFTK1 and hsa_circ_102229 or miR-152-3p was analyzed. (F) The effect of miR-152-3p and hsa_circ_102229 on PFTK1 expression was determined by western blotting. SUM149PT cells were co-transfected with circRNA or vector and miR-152-3p mimic or NC-mimic. MDA-MB-468 cells were co-transfected with circRNAsh1# or scramble and miR-152-3p inhibitor or NC-inhibitor. Data are expressed as the mean ± SD. $^{**}p < 0.01$, $^{***}p < 0.001$ and $^{\#\#\#}p < 0.001$ represent a statistically significant difference

MDA-MB-468 cells transfected with circRNAsh1# or its control (sh-NC) plasmid. The expression of hsa_circ_102229, miR-152-3p and PFTK1 mRNA was first determined in tumor tissues by qRT-PCR. As shown in Figure 7A, after inhibition of hsa_circ_102229, the expression of hsa_circ_102229, PFTK1 was down-regulated ($p < 0.001$), whereas the expression of miR-152-3p was up-regulated ($p < 0.001$). Then, the volume and weight of tumors were measured. The results showed that tumor volume and weight were smaller and lighter in the circRNAsh1# group compared to the sh-NC group ($p < 0.01$) (Figure 7B). Next, lung metastasis was measured, as shown in Fig, 7C. The images show that lung metastasis was much worse in the control group compared to that in the hsa_circ_102229 knockdown group. Subsequently, the metastatic focus and the results of morphological changes are shown in Figure 7D. The metastatic focus was remarkably

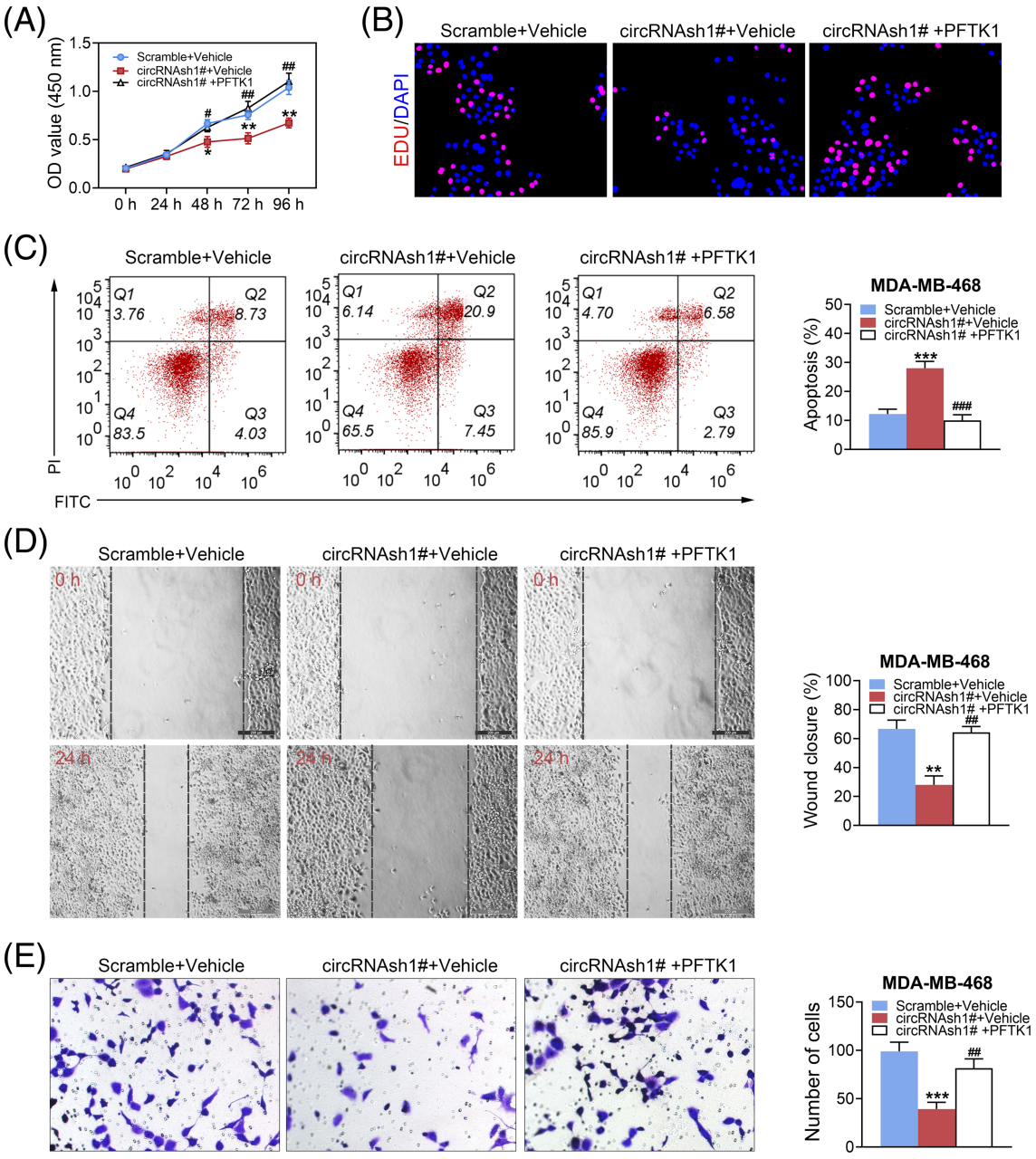

FIGURE 6 Hsa_circ_102229 promoted the proliferation, migration and invasion of TNBC cells by regulating PFTK1. MDA-MB-468 cells were co-transfected with circRNAsh1# or its control (scramble) and pcDNA3.1(+) PFTK1 or its control (vehicle). (A) MDA-MB-468 cells viability was tested by the CCK-8 assay. (B) MDA-MB-468 cells proliferation was determined by EdU staining. (C) MDA-MB-468 cells apoptosis was tested by flow cytometry. (D,E) MDA-MB-468 cells migration and invasion were detected by a wound healing assay and a transwell assay. Data are expressed as the mean ± SD. $^{*}p < 0.05$, $^{**}p < 0.01$, $^{***}p < 0.001$; $^{\#}p < 0.05$, $^{\#\#}p < 0.01$ and $^{\#\#\#}p < 0.001$ represent a statistically significant difference

reduced in the hsa_circ_102229 knockdown group ($p < 0.01$). In addition, an IHC assay was performed to determine the expression of PFTK1, Ki-67 and E-cadherin. We found that the expression of Ki-67 and PFTK1 was significantly decreased in the hsa_circ_102229 knockdown group. However, the expression of E-cadherin had the opposite tendency ($p < 0.001$) (Figure 7E). Finally, the results of TUNEL staining showed that cell apoptosis can be enhanced by suppression of hsa_circ_102229 ($p < 0.01$) (Figure 7F).

4 | DISCUSSION

With the development of advanced sequencing technologies, circRNAs have been increasingly discovered and have attracted much attention.[18,25] To date, more than 10,000 different circRNAs have been identified in various species.[26] As novel gene regulators, circRNAs are usually highly conserved across species, follow certain expression patterns and exert their functions at the

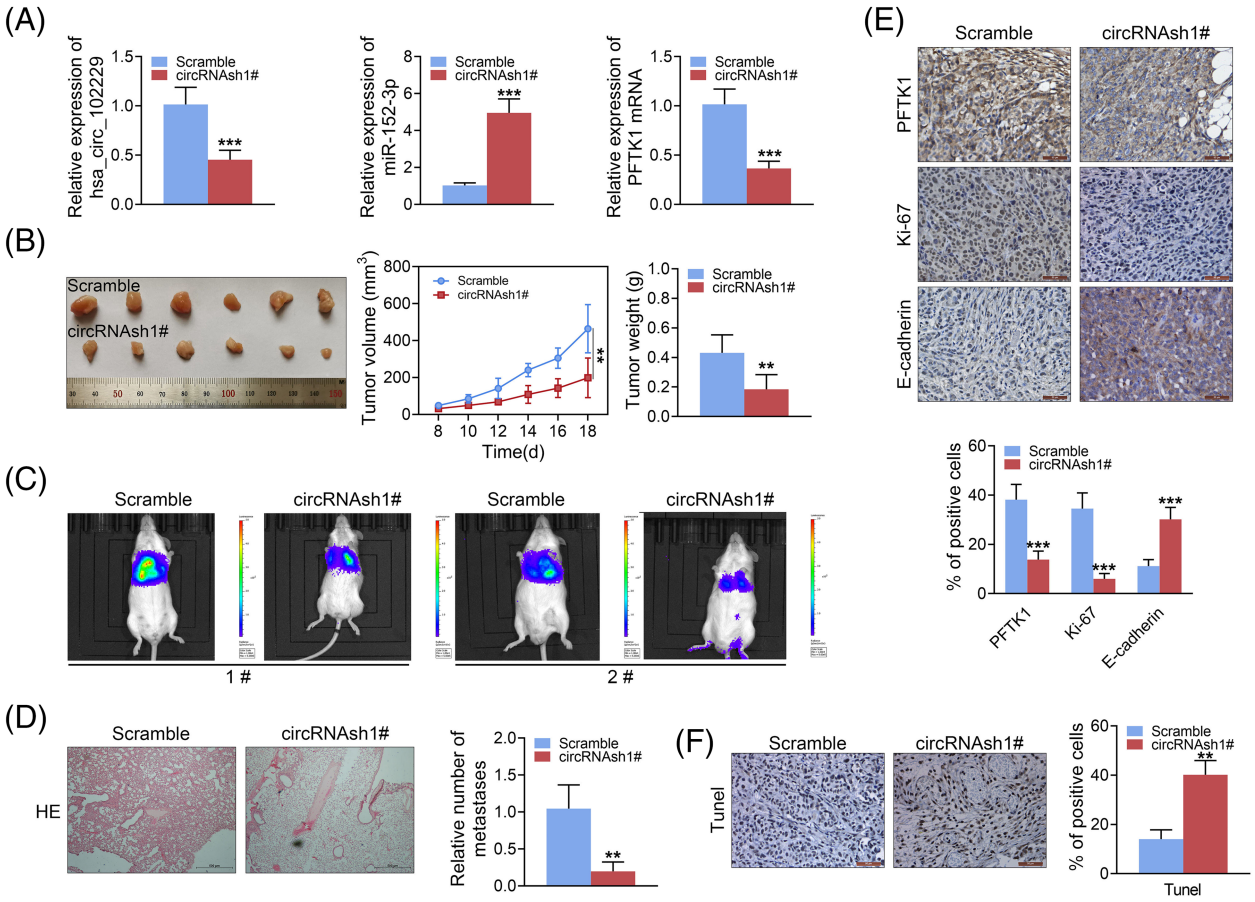

FIGURE 7 Knockdown of hsa_circ_102229 inhibited tumor growth and lung metastasis *in vivo*. (A) Mice were injected with MDA-MB-468 cells which were transfected with sh-hsa_circRNA_102229 or sh-NC. The expression of hsa_circ_102229, miR-152-3p and PFTK1 in tumor tissue from different groups of mice was tested by qRT-PCR. (B) The effects of hsa_circ_102229 knockdown on tumor volume curve and tumor weight were analyzed. (C) Lung metastasis in scramble group or hsa_circ_102229 knockdown group was detected by *in vivo* images. (D) Hemotoxylin and eosin staining of pulmonary nodules from different groups of mice is shown. (E) The expression of PFTK1, Ki67, E-cadherin in different groups was determined by IHC. (F) TUNEL staining was performed to detect apoptotic cells in different groups. Data are expressed as the mean ± SD. $^{**}p < 0.01$, $^{***}p < 0.001$ represent a statistically significant difference

post-transcriptional or transcriptional level.[27] Accumulating studies have reported that circRNAs could participate in different stages of TNBC.[23,24,28–30] However, many questions related to their functions remain unanswered. In the present study, using microarray analysis, many significantly up-regulated or down-regulated circRNAs in TNBC tissues were identified. Among them, hsa_circRNA_102229 was one of the most remarkably up-regulated circRNAs in the dataset. Moreover, survival analysis indicated that high level of hsa_circRNA_102229 was correlated with the poor clinical prognosis of patients with TNBC. Thus, further experiments were focused on hsa_circRNA_102229.

To further understand the potential role of hsa_circRNA_102229 in the progression of TNBC, hsa_circ_102229 knockdown and an overexpression system were established in SUM149PT and MDA-MB-468 cell lines, respectively. At the functional level, results indicated that hsa_circ_102229 could promote the proliferation, migration and invasion of TNBC cells, but inhibit apoptosis. Thus, we concluded that hsa_circ_102229 may play a tumor promoter role in TNBC. To understand the underlying mechanisms, bioinformatics tools were introduced. By analyzing the Starbase database, we found that miR-152-3p could be a potential binding target of hsa_circ_102229. Unlike circular RNAs, miRNAs are another type of endogenous non-coding RNAs with a length of around 22 nucleotides.[31] Although they have no protein-coding abilities, many cancer-related biological processes can be regulated by miRNAs.[32] In recent years, many miRNAs have been confirmed to be involved in the TNBC pathological process. For example, circulating miRNA-200c was expressed to a lower extent in patients with TNBC.[33] By regulating SETBP1, miRNA-211-5p could attenuate the metastasis of TNBC cells.[34] In the present study, the expression of miR-152-3p can be significantly affected by hsa_circ_102229. Furthermore, the results of a dual-luciferase assay demonstrated that hsa_circ_102229 was a direct target of miR-152-3p.

The serine/threonine-protein kinase PFTAIRE 1 (PFTK1), also known as cyclin-dependent kinase 14 (CDK14), is considered to be an important regulator of cyclins and the cell cycle.[35,36] As a member of

the Cdc2-related serine/threonine protein kinase family, PFTK1 is enriched in different tissues and cells (e.g. pancreas, brain, kidney).[37–39] It has been demonstrated that PFTK1 usually plays a tumor promoter role. For example, a study by Yang *et al*.[40] demonstrated that PFTK1 could promote the proliferation, migration and invasion of gastric cancer cells. Another study showed that knockdown of PFTK1 could inhibit proliferation, invasion and epithelial–mesenchymal transition in colon cancer cells.[41] miR-152-3p and PFTK1 were selected as downstream molecules of hsa_circ_102229 based on studies showing that miR-152-3p and PFTK1 are associated with breast cancer.[42,43] In the present study, PFTK1 was confirmed as a direct target of miR-152-3p. In line with the previous results of above studies, overexpression of PFTK1 could compromise the inhibitory effects of hsa_circ_102229, suggesting that hsa_circ_102229 could promote the proliferation, migration and invasion of TNBC cells by regulating PFTK1.

In recent years, the hypothesis of competing endogenous RNA (ceRNA) has been widely confirmed.[44] How RNAs communicate with each other by competing and binding to miRNAs and target mRNAs has been described.[44,45] In the present study, hsa_circ_102229 served as a ceRNA for miR-152-3p to modulate the expression of PFTK1. Furthermore, knockdown of hsa_circ_102229 could suppress the metastasis in animal model.

Taken together, the results of the present study indicate that hsa_circ_102229 was remarkably up-regulated in TNBC tissues and correlated with the prognosis of TNBC patients. Moreover, the functions of TNBC cells can be modulated by hsa_circ_102229. In sum, hsa_circ_102229 functions as a ceRNA for miR-152-3p to regulate PFTK1 expression.

ACKNOWLEDGEMENTS

This work was supported by the Joint Construction Project of Henan Medical Science and Technology Research Plan (Grant No. LHGJ20190146), Guidance Plan of Key Scientific Research Projects in Henan Province (Grant No. 20B320026) and Joint Project of Henan Province and Ministry (Grant No.2018010002).

CONFLICT OF INTEREST

The authors declare that they have no conflicts of interest.

AUTHOR CONTRIBUTIONS

CD and JZ designed the study and also supervised the data collection and the analysis of the data. LZ wrote this manuscript. YZ, YW and JL were responsible for data collection and analysis. All authors have read and approved the final version of the manuscript submitted for publication.

ETHICAL APPROVAL

Ethical approval was obtained from the Ethics Committee of the Ethical Committee of The First Affiliated Hospital of Zhengzhou University (Approval no. 2019-KY-291). Written informed consent was obtained from a legally authorized representative(s) for anonymized patient information to be published in this article.

DATA AVAILABILITY STATEMENT

All data generated or analyzed during this study are included in this published article.

ORCID

Jingruo Li https://orcid.org/0000-0002-1369-9995

REFERENCES

1. DeSantis CE, Ma J, Goding Sauer A, Newman LA, Jemal A. Breast cancer statistics, 2017, racial disparity in mortality by state. *CA Cancer J Clin*. 2017;67(6):439-448. https://doi.org/10.3322/caac.21412
2. Tao Z, Shi A, Lu C, Song T, Zhang Z, Zhao J. Breast cancer: epidemiology and etiology. *Cell Biochem Biophys*. 2015;72(2):333-338. https://doi.org/10.1007/s12013-014-0459-6
3. Hortobagyi GN, de la Garza SJ, Pritchard K, et al. The global breast cancer burden: variations in epidemiology and survival. *Clin Breast Cancer*. 2005;6(5):391-401. https://doi.org/10.3816/cbc.2005.n.043
4. Verma R, Bowen RL, Slater SE, Mihaimeed F, Jones JL. Pathological and epidemiological factors associated with advanced stage at diagnosis of breast cancer. *Br Med Bull*. 2012;103(1):129-145. https://doi.org/10.1093/bmb/lds018
5. Anderson WF, Chatterjee N, Ershler WB, Brawley OW. Estrogen receptor breast cancer phenotypes in the Surveillance, Epidemiology, and End Results database. *Breast Cancer Res Treat*. 2002;76(1):27-36. https://doi.org/10.1023/a:1020299707510
6. Perou CM, Sørlie T, Eisen MB, et al. Molecular portraits of human breast tumours. *Nature*. 2000;406(6797):747-752. https://doi.org/10.1038/35021093
7. Morris GJ, Naidu S, Topham AK, et al. Differences in breast carcinoma characteristics in newly diagnosed African-American and Caucasian patients: a single-institution compilation compared with the National Cancer Institute's Surveillance, Epidemiology, and End Results database. *Cancer*. 2007;110(4):876-884. https://doi.org/10.1002/cncr.22836
8. Cadoo KA, Fornier MN, Morris PG. Biological subtypes of breast cancer: current concepts and implications for recurrence patterns. *Quart J Nucl Med Mol Imag*. 2013;57(4):312-321.
9. Dent R, Trudeau M, Pritchard KI, et al. Triple-negative breast cancer: clinical features and patterns of recurrence. *Clin Cancer Res*. 2007;13(15 Pt 1):4429-4434. https://doi.org/10.1158/1078-0432.Ccr-06-3045
10. Morris PG, Murphy CG, Mallam D, et al. Limited overall survival in patients with brain metastases from triple negative breast cancer. *Breast J*. 2012;18(4):345-350. https://doi.org/10.1111/j.1524-4741.2012.01246.x
11. Dent R, Hanna WM, Trudeau M, Rawlinson E, Sun P, Narod SA. Pattern of metastatic spread in triple-negative breast cancer. *Breast Cancer Res Treat*. 2009;115(2):423-428. https://doi.org/10.1007/s10549-008-0086-2
12. Jitariu AA, Cîmpean AM, Ribatti D, Raica M. Triple negative breast cancer: the kiss of death. *Oncotarget*. 2017;8(28):46652-46662. https://doi.org/10.18632/oncotarget.16938
13. Memczak S, Jens M, Elefsinioti A, et al. Circular RNAs are a large class of animal RNAs with regulatory potency. *Nature*. 2013;495(7441):333-338. https://doi.org/10.1038/nature11928
14. Li P, Chen S, Chen H, et al. Using circular RNA as a novel type of biomarker in the screening of gastric cancer. *Clin Chim Acta*. 2015;444:132-136. https://doi.org/10.1016/j.cca.2015.02.018
15. Cocquerelle C, Mascrez B, Hétuin D, Bailleul B. Mis-splicing yields circular RNA molecules. *FASEB J*. 1993;7(1):155-160. https://doi.org/10.1096/fasebj.7.1.7678559

16. Salzman J, Gawad C, Wang PL, Lacayo N, Brown PO. Circular RNAs are the predominant transcript isoform from hundreds of human genes in diverse cell types. *PLoS ONE*. 2012;7(2):e30733. https://doi.org/10.1371/journal.pone.0030733
17. Salzman J, Chen RE, Olsen MN, Wang PL, Brown PO. Cell-type specific features of circular RNA expression. *PLoS Genet*. 2013;9(9):e1003777. https://doi.org/10.1371/journal.pgen.1003777
18. Zhang Y, Zhang XO, Chen T, et al. Circular intronic long noncoding RNAs. *Mol Cell*. 2013;51(6):792-806. https://doi.org/10.1016/j.molcel.2013.08.017
19. Meng S, Zhou H, Feng Z, et al. CircRNA: functions and properties of a novel potential biomarker for cancer. *Mol Cancer*. 2017;16(1):94. https://doi.org/10.1186/s12943-017-0663-2
20. Bi W, Huang J, Nie C, et al. CircRNA circRNA_102171 promotes papillary thyroid cancer progression through modulating CTNNBIP1-dependent activation of β-catenin pathway. *J Exp Clin Cancer Res*. 2018;37(1):275. https://doi.org/10.1186/s13046-018-0936-7
21. Chen D, Ma W, Ke Z, Xie F. CircRNA hsa_circ_100395 regulates miR-1228/TCF21 pathway to inhibit lung cancer progression. *Cell Cycle*. 2018;17(16):2080-2090. https://doi.org/10.1080/15384101.2018.1515553
22. Liu Z, Mi M, Li X, Zheng X, Wu G, Zhang L. lncRNA OSTN-AS1 may represent a novel immune-related prognostic marker for triple-negative breast cancer based on integrated analysis of a ceRNA network. *Front Genet*. 2019;10:850. https://doi.org/10.3389/fgene.2019.00850
23. Chen B, Wei W, Huang X, et al. circEPSTI1 as a prognostic marker and mediator of triple-negative breast cancer progression. *Theranostics*. 2018;8(14):4003-4015. https://doi.org/10.7150/thno.24106
24. Yang R, Xing L, Zheng X, Sun Y, Wang X, Chen J. The circRNA circAGFG1 acts as a sponge of miR-195-5p to promote triple-negative breast cancer progression through regulating CCNE1 expression. *Mol Cancer*. 2019;18(1):4. https://doi.org/10.1186/s12943-018-0933-7
25. Cooper DA, Cortés-López M, Miura P. Genome-wide circRNA profiling from RNA-seq data. *Methods Mol Biol*. 2018;1724:27-41. https://doi.org/10.1007/978-1-4939-7562-4_3
26. Chen LL, Yang L. Regulation of circRNA biogenesis. *RNA Biol*. 2015;12(4):381-388. https://doi.org/10.1080/15476286.2015.1020271
27. Salzman J, Circular RNA. Expression: its potential regulation and function. *Trends Genet*. 2016;32(5):309-316. https://doi.org/10.1016/j.tig.2016.03.002
28. Tang H, Huang X, Wang J, et al. circKIF4A acts as a prognostic factor and mediator to regulate the progression of triple-negative breast cancer. *Mol Cancer*. 2019;18(1):23. https://doi.org/10.1186/s12943-019-0946-x
29. Wang ST, Liu LB, Li XM, et al. Circ-ITCH regulates triple-negative breast cancer progression through the Wnt/β-catenin pathway. *Neoplasma*. 2019;66(2):232-239. https://doi.org/10.4149/neo_2018_180710N460
30. Sang M, Meng L, Liu S, et al. Circular RNA ciRS-7 maintains metastatic phenotypes as a ceRNA of miR-1299 to target MMPs. *Mol Cancer Res*. 2018;16(11):1665-1675. https://doi.org/10.1158/1541-7786.Mcr-18-0284
31. Rupaimoole R, Slack FJ. MicroRNA therapeutics: towards a new era for the management of cancer and other diseases. *Nat Rev Drug Discov*. 2017;16(3):203-222. https://doi.org/10.1038/nrd.2016.246
32. Van Roosbroeck K, Calin GA. Cancer hallmarks and microRNAs: the therapeutic connection. *Adv Cancer Res*. 2017;135:119-149. https://doi.org/10.1016/bs.acr.2017.06.002
33. Niedźwiecki S, Piekarski J, Szymańska B, Pawłowska Z, Jeziorski A. Serum levels of circulating miRNA-21, miRNA-10b and miRNA-200c in triple-negative breast cancer patients. *Ginekol pol*. 2018;89(8):415-420. https://doi.org/10.5603/GP.a2018.0071
34. Chen LL, Zhang ZJ, Yi ZB, Li JJ. MicroRNA-211-5p suppresses tumour cell proliferation, invasion, migration and metastasis in triple-negative breast cancer by directly targeting SETBP1. *Br J Cancer*. 2017;117(1):78-88. https://doi.org/10.1038/bjc.2017.150
35. Malumbres M, Harlow E, Hunt T, et al. Cyclin-dependent kinases: a family portrait. *Nat Cell Biol*. 2009;11(11):1275-1276. https://doi.org/10.1038/ncb1109-1275
36. Lazzaro MA, Julien JP. Chromosomal mapping of the PFTAIRE gene, Pftk1, a cdc2-related kinase expressed predominantly in the mouse nervous system. *Genomics*. 1997;42(3):536-537. https://doi.org/10.1006/geno.1997.4760
37. Yang T, Chen JY. Identification and cellular localization of human PFTAIRE1. *Gene*. 2001;267(2):165-172. https://doi.org/10.1016/s0378-1119(01)00391-2
38. Fan S, Zhao C, Zhang L, et al. Knockdown of PFTK1 inhibits the migration of glioma cells. *J Mol Neurosci*. 2015;57(2):257-264. https://doi.org/10.1007/s12031-015-0600-z
39. Anderson JC, Willey CD, Mehta A, et al. High Throughput Kinomic Profiling Of Human Clear Cell Renal Cell Carcinoma Identifies Kinase Activity Dependent Molecular Subtypes. *PLoS ONE*. 2015;10(9):e0139267. https://doi.org/10.1371/journal.pone.0139267
40. Yang L, Zhu J, Huang H, et al. PFTK1 promotes gastric cancer progression by regulating proliferation, migration and invasion. *PLoS ONE*. 2015;10(10):e0140451. https://doi.org/10.1371/journal.pone.0140451
41. Zhu J, Liu C, Liu F, Wang Y, Zhu M. Knockdown of PFTAIRE protein kinase 1 (PFTK1) inhibits proliferation, invasion, and EMT in colon cancer cells. *Oncol Res*. 2016;24(3):137-144. https://doi.org/10.3727/096504016x14611963142218
42. Song Y, Zhang M, Lu MM, et al. EPAS1 targeting by miR-152-3p in paclitaxel-resistant breast cancer. *J Cancer*. 2020;11(19):5822-5830.
43. Gu X, Wang Y, Wang H, et al. Upregulated PFTK1 promotes tumor cell proliferation, migration, and invasion in breast cancer. *Med Oncol*. 2015;32(7):195.
44. Tay Y, Rinn J, Pandolfi PP. The multilayered complexity of ceRNA crosstalk and competition. *Nature*. 2014;505(7483):344-352. https://doi.org/10.1038/nature12986
45. Zhong Y, Du Y, Yang X, et al. Circular RNAs function as ceRNAs to regulate and control human cancer progression. *Mol Cancer*. 2018;17(1):79. https://doi.org/10.1186/s12943-018-0827-8

SUPPORTING INFORMATION

Additional supporting information may be found online in the Supporting Information section at the end of this article.

How to cite this article: Du C, Zhang J, Zhang L, Zhang Y, Wang Y, Li J. Hsa_circRNA_102229 facilitates the progression of triple-negative breast cancer via regulating the miR-152-3p/PFTK1 pathway. *J Gene Med*. 2021;23(9):e3365. https://doi.org/10.1002/jgm.3365